Investigation of Neuregulin-1 Treatment in 3D engineered skeletal muscle toward Intrafusal Spindle Fiber Generation *in vitro*

Cecelia Jean Watson

A thesis

submitted in partial fulfillment of the

requirements for the degree of

Master of Science

University of Washington

2023

Committee:
David Mack
Alec Smith
Micheal Regnier

Program Authorized to Offer Degree:

Bioengineering

University of Washington

Abstract

Investigation of Neuregulin-1 Treatment in 3D engineered skeletal muscle toward Intrafusal Spindle Fiber Generation *in vitro*

Cecelia Jean Watson
Chair of the Supervisory Committee:
David Mack
Department of Rehabilitation Medicine

Abstract: Intrafusal fibers of the muscle spindle play an essential role in the reflex circuits that regulate muscle contraction in response to strain. Muscle spindle dysfunction is suggested to contribute to the impaired proprioception and ataxic behavior seen in muscular dystrophies and other neuromuscular disorders. The molecular mechanism by which these disorders impair muscle spindle function has yet to be determined. This is partly due to the scarcity of intrafusal fibers in the body and the difficulty of isolating them via biopsy. This limited availability of muscle spindle models has led to a lack of study of these structures in neuromuscular research. Research regarding the muscle spindle and intrafusal fibers to-date has largely relied on murine cells. In the small body of work so far performed using human cells, de novo generation of intrafusal fibers has only been attempted in 2D for short periods of time. This project used new technology to create 3D engineered muscle tissues (EMTs) from human induced pluripotent stem cells and investigated the effects of treatment with Neuregulin-1, which is known to drive intrafusal fiber formation *in vivo*. The effect of Neuregulin-1 treatment was characterized using immunofluorescence and longitudinal analysis of EMT contraction kinetics. This research represents a new model for studying intrafusal fiber and muscle spindle generation, the first to thoroughly investigate previously published differentiation protocols in 3D for over 30 days and provides the most in-depth analysis of intrafusal fiber formation in vitro to-date.

Introduction

Proprioception can be defined as the perception of position in the body, which is exceedingly important to help with posture and coordinated movement [1]. Improper proprioception can lead to varying degrees of impairment, leaving some with severely limited voluntary movement. Decline in proprioception is a marker of many neuromuscular diseases, such as muscular dystrophies and arthrogryposis multiplex congenita [40,41]. Proprioception is driven by muscle spindles, which are essentially small stretch receptors found within muscles.

Muscle spindles are made of both intrafusal and extrafusal fibers encased in a capsular structure, and are innervated by primary (Ia) and secondary (II) afferent sensory neurons as well as efferent γ-motor neurons [2]. The intrafusal fibers within the spindle are specialized to report the changes in muscle length, as well as the velocity at which the length is changing, to the central nervous system. Though muscle spindles play an important role in the neuromuscular reflex arc, they are relatively rare with estimates suggesting there are ~50,000 in the human body. This limited muscle spindle availability has led researchers away from muscle spindles and instead to creating various *in vitro* and *in vivo* models of various neuromuscular disorders to study proprioception [3].

To create better disease models, it is highly important to consider how the structures of interest develop naturally *in vivo*, to see if researchers can mimic the process. During fetal development, when Type 1a and Type 2 sensory neuron axons contact myotubes, they release a molecule called Neuregulin-1 (NRG1) which then activates ErbB2/3 receptors on myotubes. This drives the expression of the transcription factor Egr3, which then drives the conversion of developing myotubes into the intrafusal fibers of muscle spindles [5-7]. NRG1 is one out of six genes in the Neuregulin family [8]. Since its discovery in 1990, NRG1 has been found to be involved in many different pathways in the body, including the pathogenesis of diseases such as schizophrenia, multiple sclerosis, and breast cancer. Within the NRG1 gene, there are six different types and alternative splicing has generated 33 different isoforms [9]. NRG1 type I, II, IV, and V isoforms have immunoglobulin (Ig)-like domains in addition to a cysteine-rich domain (CRD), whereas other forms only have the CRD. In early muscle spindle research, it was found that Ig-containing isoforms of NRG1 are preferentially expressed by proprioceptive sensory neurons and can induce spindle morphogenesis [10]. In addition, within NRG1-Type 1 there are also α and β isoforms [11]. The NRG1-β1 isoform has been found to be 10x more active, and is commonly used in in vitro muscle spindle research to date [11,35-39].

In 2004, the Jacobson lab group used NRG1 to induce the expression of Egr3 at an mRNA and protein level in a 2D human primary myoblasts [12]. Their results showed NRG1 treated cells showed an increase in the expression of muscle spindle-specific slow developmental myosin. More recent work has shown there are established techniques for creating extrafusal muscle spindle fibers from human iPSCs [13]. In 2017, the Hickman lab group in Florida first attempted to derive intrafusal muscle spindle fibers from human satellite cells [14]. In 2020, this group published a second paper in which they characterized a system of stem cell derived motor neurons and satellite cell derived ‘intrafusal muscle fibers’ by functionally testing the co-cultures

with electrical stimulation [15]. The group published a third paper in 2020, in which they attempted to promote intrafusal fiber development from an iPSC cell line. Their results showed that iPSCs treated with NRG1 showed an increase in bag-fiber morphologies and increased positive stains for S46 and pErbB2, which are said to be the most specific intrafusal fiber specific markers [16-19].

The papers discussed above claim to demonstrate a protocol for generating functional intrafusal fibers from iPSCs, but my PI and I both disagree. Their work bases intrafusal fiber identification on bag-like morphology and mainly S46 (Myosin Heavy Chain 6) staining. Extrafusal fibers can also demonstrate this morphology, and intrafusal fibers can also be linear, so bag fiber morphology alone is not the best indication of intrafusal fibers being created. It should also be noted that there are three subtypes of intrafusal muscle spindle fibers; nuclear bag1, bag2 and chain, where there are commonly 2–3 bag fibers and 4–6 chain fibers per spindle [20]. The work performed by the Hickman group does not account for or attempt to differentiate between these different fiber types. We also do not believe that the activation of motor neurons shown in the second paper provides adequate proof of functionality. In order to demonstrate true functionality of these fibers, it must be demonstrated that there is activation in response to mechanical stretch rather than contraction in response to stimulation. Lastly, their differentiations last up to a maximum of 18 days, which we do not believe is adequate for proper intrafusal fiber structure to form.

Overall, their work provides a clear basis that NRG1 treatment appears to promote a shift toward an intrafusal fiber phenotype, shown by increased number of bag fibers as well as some immunohistochemistry data to support this. There is a clear gap in this work, though, regarding how replicable these experiments are in iPSCs, how would these experiments work in the 3D space, and how exactly does this differentiation treatment affect the functional output of treated cells. While the full timeline and mechanism of muscle spindle development is unknown, it is clear that the cells receive multiple external cues and have many different cell type interactions that guide the differentiation in vivo [21-25]. A 3D environment is a much better model of these conditions in vivo as it offers cells the ability to receive cues from their extracellular matrix in multiple directions [20]. It has also been seen that 3D muscle cultures tend to produce more mature adult cells than in 2D.

This thesis aims to address some of these questions and provide valuable preliminary data for the Mack Lab to eventually develop a complete neuromuscular reflex arc in-a-dish. In collaboration with scientists from the Mack Lab, CuriBio developed a platform called Mantarray™ for the generation of 3D Engineered Muscle Tissues (EMTs) **Fig#1**. This platform uses a magnetic measurement system to directly measure the contractility of up to 24 EMTs simultaneously, over multiple weeks. This technology allowed me to monitor the contractility of EMTs during various time points during NRG1-mediated intrafusal spindle fiber differentiation experiments, using human-derived iPSCs, and compare those results to those undergoing an extrafusal fiber differentiation. In addition to this, I was able to test antibodies found by previous groups to be intrafusal fiber specific on the EMTs as well as in rat muscle tissue.

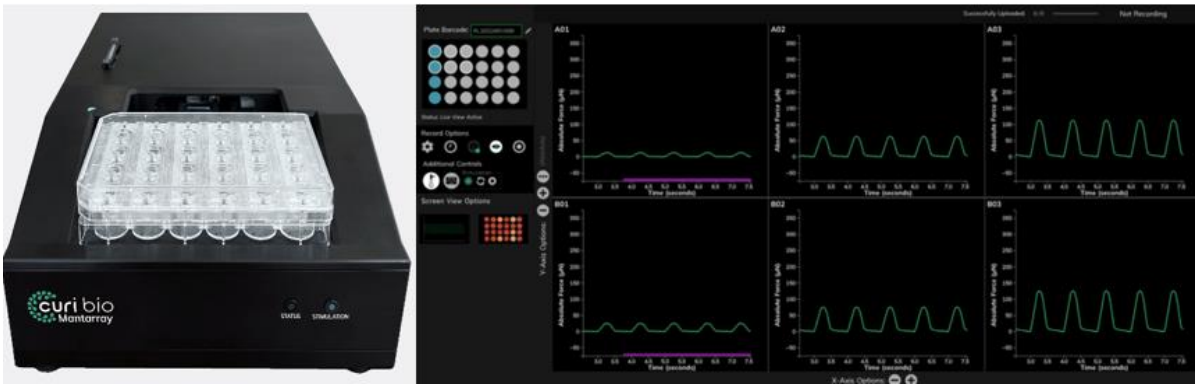

Fig #1: Image of CuriBio's Mantarray System (left) and sample readout (right). Image from CuriBio's website found here.

Methods

Staining Protocol

Soleus Section Stains: Slides containing soleus sections were received from the histology core, then deparaffinized using Xylene washes, ethanol washes at 100%, 90%, 80%, and 70%, then placed in a 95°C citrate buffer for 30 minutes, or until they cooled down to 50°C for antigen rescue. Blocking solution was applied (DPBS + 0.2% Triton X-100 + 1% BSA) and left to rest for 30 minutes at RT. Primary antibody solution (DPBS + 1% BSA + ab1 + ab2) was applied and left overnight at 4°C. The slides were washed with DPBS three times for 10 minutes, then the secondary antibody solution (PBS + 1:1000 DAPI + 1:500 ab1 + 1:500 ab2) to each slide and incubated for 1 hour RT. Washes were repeated and coverslips were applied. A hydrophobic barrier PAP pen was used to isolate soleus sections on the slides, to ensure the primary and secondary antibody solutions applied would not wash off the slides.

2D stains: Cells were fixed using 4% PFA in PBS for 15 minutes. After fixing, the cells were permeabilized using 0.2% Triton-X 100 for 15 minutes and then immersed in a blocking solution of 0.5% BSA for one hour. The cells were then incubated with a primary antibody diluted in the blocking solution overnight. The next day the cells were washed multiple times with PBS to remove and non-specific binding proteins and then incubated with a corresponding secondary antibody for two hours. Lastly, the cells were incubated in a DAPI and PBS working solution (at a concentration of 1:1000) for 15 minutes then washed with PBS three more times before imaging.

3D EMT Stains: Make a blocking buffer (500ul-1mL for each EMT) consisting of 1x Perm Wash (from 10x stock solution) 0.3% TritonX-100, 1% BSA (bovine serum albumin, solid crystals), 1% donkey** serum (frozen) in 1x PBS. EMTSs were submerged in the blocking buffer and placed in a shaker incubator (38°C, 150 speed), overnight. Next, EMTs were submerged in a primary antibody solution consisting of the primary antibodies [ab1 1:100, ab2 1:100, etc.] and 5% DMSO in the blocking buffer, and placed in shaker incubator (38°C, 150 speed) for 24 hours. Next, the EMTs were submerged in a wash buffer consisting of 0.3% TritonX-100 0.5% 1-thioglycerol in PBS and placed in a shaker incubator (38°C, 150 speed), for 2 hours (this is repeated twice). Next EMTs are submerged in a secondary antibody solution, which is the same as the primary antibody solution, except the secondaries are used at a concentration of 1:400. These are left in the shaker incubator (38°C, 150 speed) overnight. The wash buffer step is repeated.

Lastly, the EMTs were submerged in a clearing solution consisting of 40% N-methyl acetamide, Histodenz (solid crystals), TritonX-100 (=0.1%), and 1-thioglycerol (=0.5%). The EMTs were submerged in the clearing solution for 48 hours at room temperature in a rotating shaker, then mounted onto slides for imaging,

		Vendor/ Catalog Number
Primary Antibodies	1. Egr3 (A7) 2. MyL2 3. S46 4. MyH6 5. MyH13 6. Pan-MyH 7. a-actinin 8. MyH7b	1. Santa Cruz Biotech / sc-390967 2. Invitrogen / PA5-54073 3. DSHB 4. MyBioSource / MBS2003392 5. MyBioSource / MBS474453 6. Invitrogen / PA5-31466 7. Thermo Fischer / MA1-22863 8. Received from collaborator
Secondary Antibodies	1. Donkey anti-mouse 488 2. Donkey anti-rabbit 594 3. Goat anti-mouse 488	1. Invitrogen / A-21202 2. Invitrogen / A-21207 3. Invitrogen / A-11001

iPSC Primary Differentiations

Differentiation of iPSCs and commitment to the myogenic lineage was achieved using a protocol modified from those published previously [33,34]. First, UCS-2 iPSCs were plated at 15,000 cells/cm^2 and grown to roughly 40% confluency in mTeSR. At this point, the medium was replaced with a differentiation medium consisting of DMEM/F12 basal medium, 1x non-essential amino acid supplement (Thermo Fisher Scientific), 1x Insulin-Transferrin-Selenium supplement (Thermo Fisher Scientific), 3 µM CHIR99021 (Axon Medchem, Reston, VA, USA), and 0.2 µg/mL LDN193189 (Miltenyi Biotec, Waltham, MA, USA). On day 3 post-induction, this medium was further supplemented with 20 ng/mL bFGF (R&D Systems, Minneapolis, MN, USA). On day 6 post-induction, the CHIR99021 and the Insulin-Tranferrin-Selenium supplement were removed and replaced with 15% knockout serum replacement (KSR; Thermo Fisher Scientific), 2 ng/mL IGF-1 (R&D Systems), and 10 ng/ mL HGF (R&D Systems). On day 8 post-induction, bFGF, HGF, and LDN193189 were all removed from the differentiation medium. On day 12 post-induction, HGF was again supplemented into medium, and this composition was then maintained until day 28. Throughout this period, medium was changed daily. On day 28 post-induction, confluent cultures were passaged using TrypLE Select and replated on Matrigel-coated surfaces for further expansion. Cells at this stage stained positive for the muscle-specific marker desmin and could be induced to fuse, forming multinuclear myotubes with distinct sarcomeric patterning. All subsequent expansion steps were performed using a commercially-sourced skeletal muscle growth medium (Lonza Group AG, Basel Switzerland) and cells were fed every 2–3 days. At day 32 post-induction, differentiated cells were again lifted off their culture surfaces using TrypLE Select and subjected to fluorescence activated cell sorting (FACS) after

being stained with an erbB3 antibody (Biolegend, San Diego, CA, USA) conjugated to phycoerythrin. FACS purification was performed with the support of the Cell Analysis Facility in the Department of Immunology at the University of Washington. Purified cultures were further expanded on Matrigel-coated plates to generate sufficiently large populations of cells for downstream experiments. All cells used in this study were isolated from passage 1 to 4 cells as analysis of desmin positivity indicated the persistence of a relatively stable myogenic fraction in these cultures through this level of expansion.

I performed multiple iPSC primary differentiation experiments, but due to time constraints of the Master's program, the skeletal muscle myoblasts used in my experiments were taken from lab stock.iPSC-derived myoblasts were plated onto Matrigel coated plastic at a density of 50k/cm^2. They were grown until confluency in Lonza skeletal muscle growth medium.

3D EMT Experiments:

Post Preparation: First the CuriBio Mantarray posts (on the lid) were prepped through the following technique: Place in 0.1% PEI for 10 minutes, wash with ddH2O for five minutes, place in 0.01% glutaraldehyde for 30 min, repeat two more five-minute ddH2O washes, then set posts face up to dry.

Plate preparation: Place the plate with casting wells on ice. Using 3ul of thrombin with 47ul of DMEM per well, coat the bottom of each casting well with the thrombin mixture ensuring the entire bottom surface is covered.

Tissue Casting: Once myoblasts have reached confluency, wash with DPBS and then add 10X TrypleE diluted in DPBS. Repeat with Lonza human dermal fibroblasts as well. Let sit for 3-5 minutes until the cells appear lifted, then add DMEM to inactivate the TrypleE and transfer cells to a falcon tube. At this point perform a cell count, then spin the cells down at 1200 RPM for five minutes. Each EMT requires 750,000 myoblasts, 75,000 fibroblasts, each in a volume of 30ul. In addition, each tissue requires 30ul of Matrigel and 10 ul of fibrinogen, to create a total seeding volume of 150 µL and a seeding density of 5 million cells/ mL. Once the number of tissues has been determined, resuspend cells in the volume of DMEM needed, and create a master mix of all necessary components in a falcon tube. Place posts into the casting wells, and add 100ul of the [well-mixed] master mix into the casting wells, making sure to (1) titrate many times to mix up the components (2) ensuring the outsides of the posts are well covered and (3) using a new pipette tip for each EMT so to not risk premature aggregation between the thrombin on the pipette tip and the fibrinogen in the master mix. Once all Tissues are cast, place in the incubator for 80 minutes. After 80 minutes add 1 mL of 2g/L aminocaproic acid (ACA) in Lonza skeletal muscle medium for 15 more minutes. Then lift posts out and transfer tissues to a new 24 well plate, filled with 2ml/well of 2g/L ACA in Lonza skeletal muscle medium. Tissues are cast on D-1 and transferred to differentiation medium on D0.

EMT Differentiation: The differentiation medium applied D0-end consists of the following: 4% ACA, 2% horse serum, 2% B27 supplement, 1% non-essential amino acids, HGF (1:1000), IGF1 (1:1000), sB (1:10,000), and +/- NRG1 (various concentrations) in high-glucose DMEM. EMTs are fed every 2-3 days until fixation in 4% PFA for 24-48 hours **(Fig#2).**

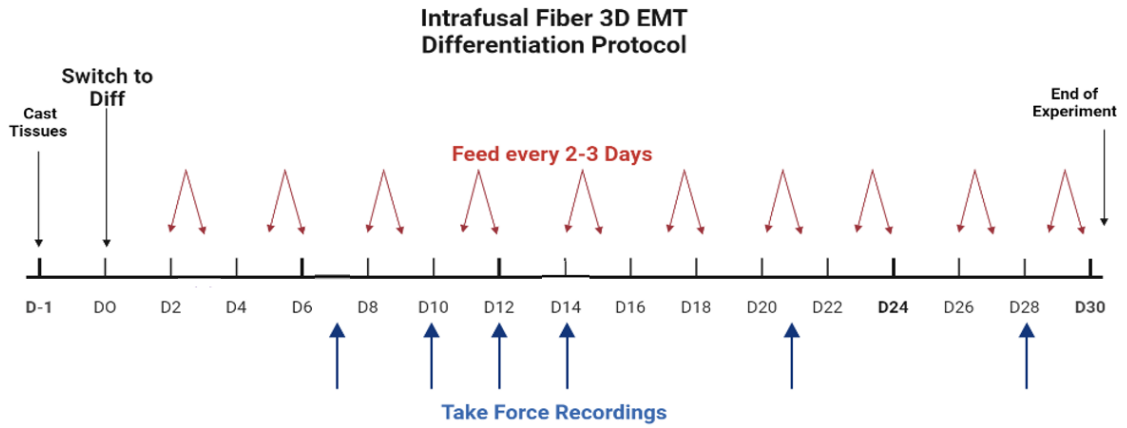

Fig #2: EMT differentiation protocol.

EMT Force Recordings and Analysis: EMT contraction was elicited via broad-field electrical stimulation. A 24-well plate lid supporting graphite electrodes that was compatible with the Mantarray hardware was used in conjunction with a C-Pace EP in-culture stimulator (IonOptix, Westwood, MA, USA). EMT cultures were subjected to electrical pulses of 10 V for 5 ms at a rate of 1 Hz for analysis of twitch contractions and 10–50 Hz to analyze tetanic responses. Post-deflection was measured by tracking the deformation of the magnetic field caused by movement of the magnet embedded in the flexible post using the dedicated Mantarray software suite. After the force recordings were measured in the Mantarray system, it outputs files which can be zipped and input into Pulse 3D software for analysis. Pulse 3D delivers data in excel sheets and further analysis was performed using PRISM software. As the described system is non-invasive, individual EMTs could be monitored for changes in function over time. For the purposes of these studies, contractile properties of cultured EMTs were measured every 4-7 days between days 7 and 31 post tissue formation.

Imaging

Images were taken on a Nikon A1 Confocal courtesy of ISCRM. Images were taken at 10x, 20x, and 60x magnification and analyzed using ImageJ software. Nuclei counting in ImageJ involved changing the image to 8-bit and binary. The color thresholding was determined using the Otsu's method option, then the watershed tool was used to separate clusters of nuclei. Then the Analyze Particles command was used, and the output was a rough estimate of either (1) the total number of nuclei if using the output from the DAPI channel or (2) the number of Egr3 positive nuclei if using the output from the FITC channel.

Image analysis

Images were opened in ImageJ software for analysis. The line tool was used to measure myotube width. To analyze sarcomere length, I followed the method described in "The scanning gradient Fourier transform (SGFT) method for assessing sarcomere organization and alignment" [32]. This method works in conjunction with MATLAB software to accurately determine the length of sarcomeres in a set of images.

Results

Aim#1: Attempt to validate intrafusal fiber specific markers *in vivo*

Due to limited research into muscle spindle development, I needed to look for antibody markers that could be used as a positive control when looking at muscle spindles *in vivo*. This way, any markers that were successful (i.e., specific), then I could use on the EMTs to test if they were becoming intrafusal fibers. After harvesting 10 soleus muscles from rats in the Mack Lab colony, they were fixed in formalin and given to the Histology Core at ISCRM for sectioning. The first stain I performed was Hematoxylin and eosin (H&E) stain to get a broad look at structure. Based on initial screening of the slides, I found multiple structure that I believed could be muscle spindles **(Fig#3).**

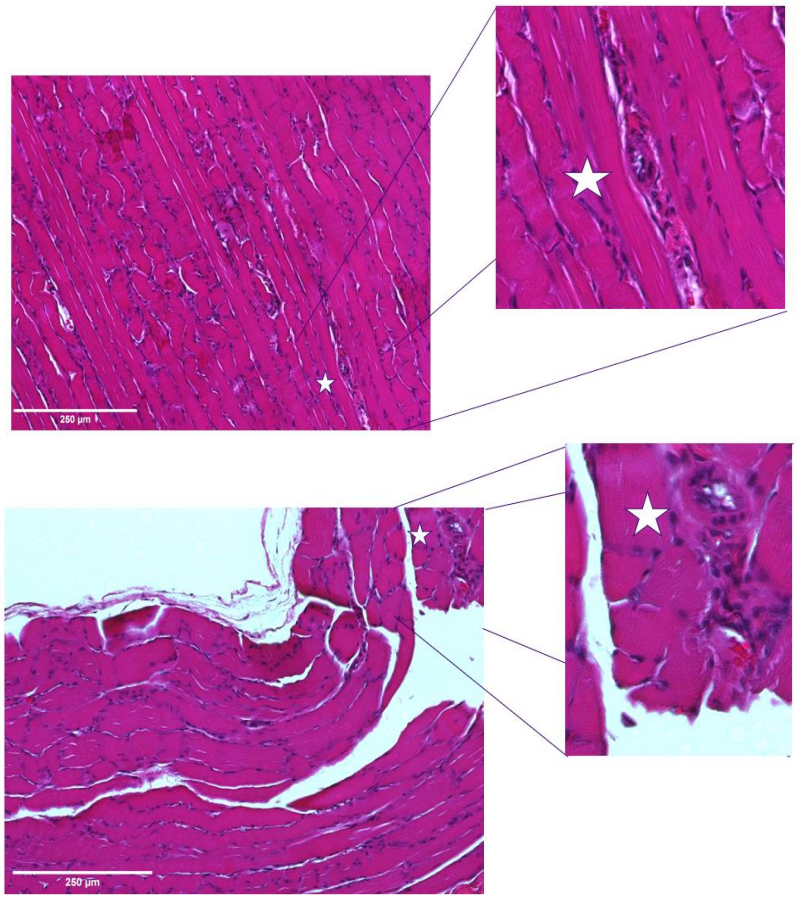

Fig #3: H&E staining of rat soleus muscle sections. Muscle spindles indicated by stars.

Based on the H&E stain, I was confident that I would be able to identify spindle structures, so I decided to move forward with testing various markers said to be intrafusal fiber specific in the literature. The first stain attempted was Myosin Light Chain 2 (MyL2) with a pan-Myosin Heavy Chain background **(Fig#4).** While there was some MyL2 positivity, there was also bright positivity on MyL2 staining throughout the myotube cross sections in a tiger-print like pattern.

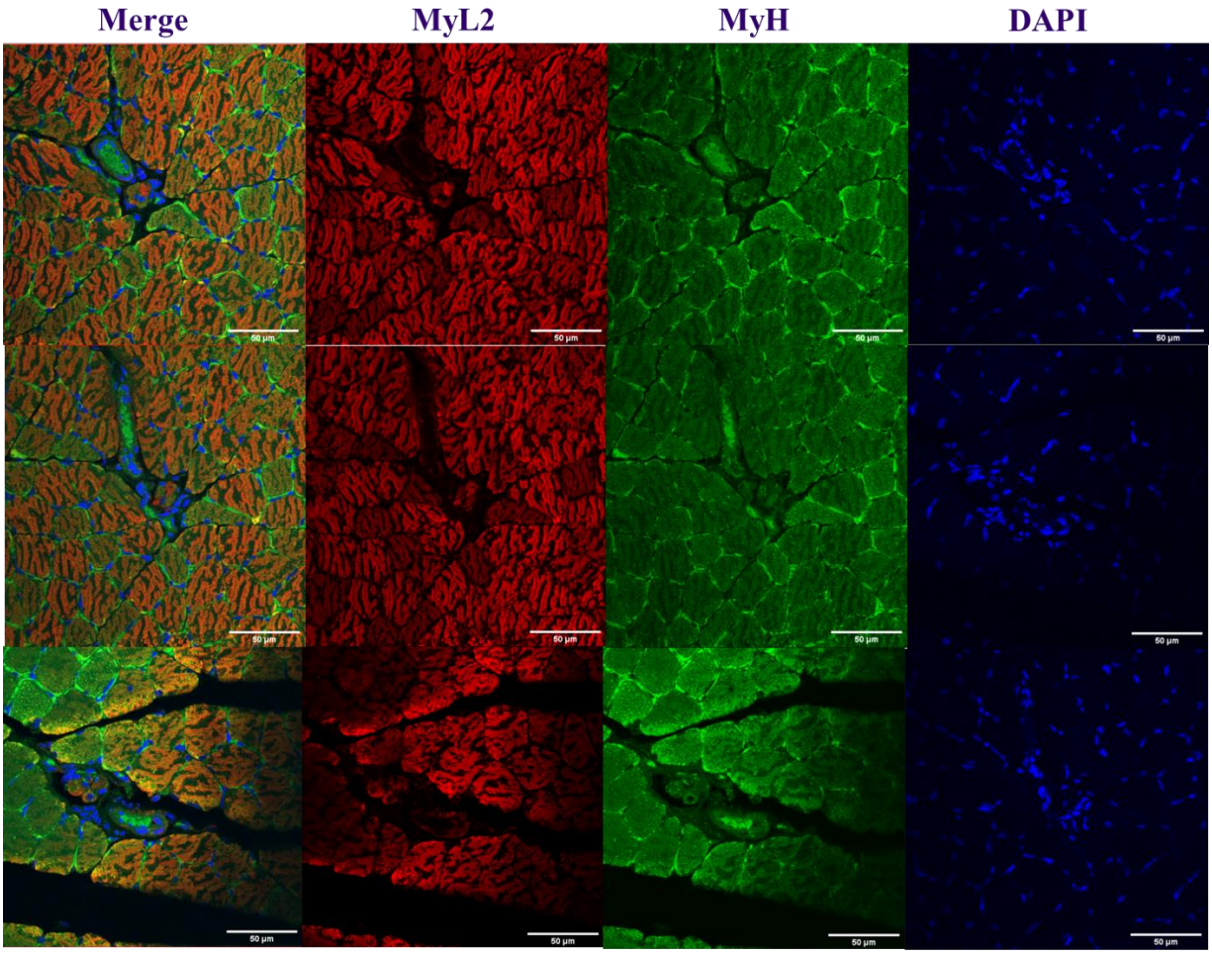

Fig #4: MyL2 and MyH staining of rat soleus muscle sections.

The next stain attempted was a Myosin Heavy Chain 6 (MyH6) antibody, a cardiac myosin, with a Myosin Heavy Chain 7 (MyH7) background stain **(Fig#5).** Again, while I saw brighter positivity in the intrafusal fiber structures in comparison to the background, I again saw that tiger-like patterned staining throughout the myotube structures in the MyH6 stain. As soleus muscles are slow twitch muscles, the myotube structures should be composed of mostly slow twitch MyH6 and MyH7. In the MyH7 stain, I do see variable positivity between myotubes,

suggesting that I am seeing some specificity with that specific antibody. Due to the strange patterns seen, I was unable to say that the MyH6 and MyL2 antibodies were specific.

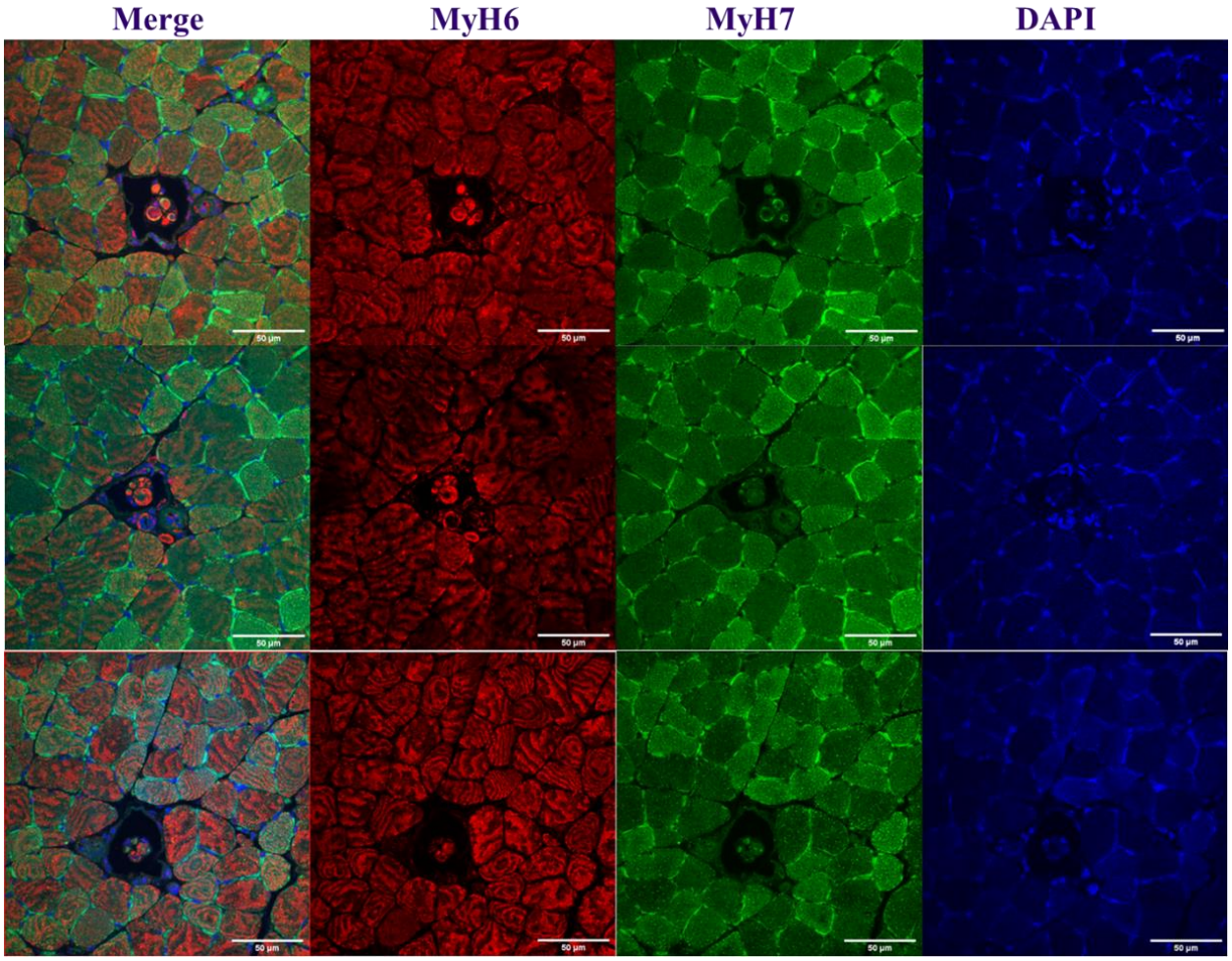

Fig #5: MyH6 and MyH7staining of rat soleus muscle sections.

I then performed another stain against MYH6, but used an antibody from another vendor that pervious groups have had success with [2,14-16, 20]. I stained the soleus sections with this S46 antibody as well as a Myosin Heavy Chain 13 (MyH13) antibody **(Fig#6).** While I did not see strange staining patterns like in the previous stains, unfortunately neither of these antibodies appeared to be specific to the intrafusal spindle fiber structures. The last stain performed was using antibodies to stain against Egr3 and MyH7b **(Fig#7).** As I had had success in the past using the Egr3 antibody, I had hoped this stain would be successful, but it along with the MyH7b stain, appeared to be non-specific.

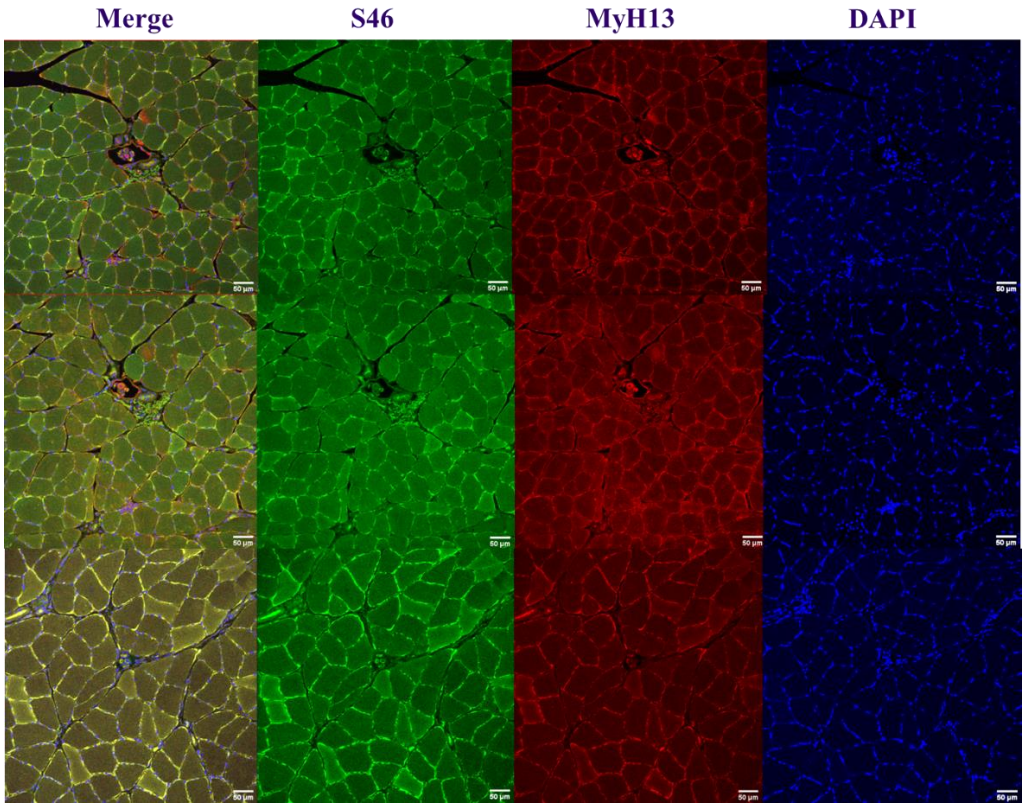

Fig #6: MyH6 (S46) and MyH13 staining of rat soleus muscle sections.

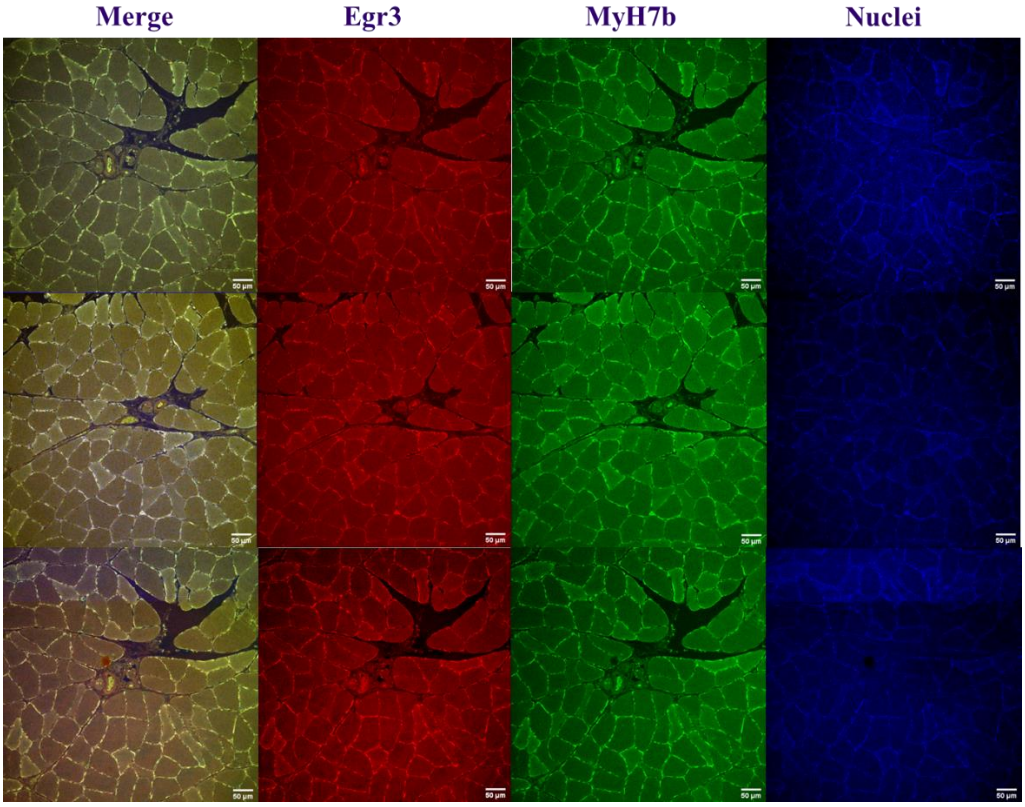

Fig #7: Egr3 and MyH7b staining of rat soleus muscle sections.

Aim#2: Characterize Neuregulin-1 treatment in 3D Engineered Muscle Tissues (EMTs)
Morphology

After maintaining the EMTs throughout the 31-day protocol, I stained them using a tissue clearing protocol as described in the methods section. The first stain attempted was using a MyH7b antibody. They were then imaged at 20x magnification **(Fig#8)** to view overall morphology on the entire tissue and then at 60x magnification **(Fig#9)** to look closer at sarcomeric structures.

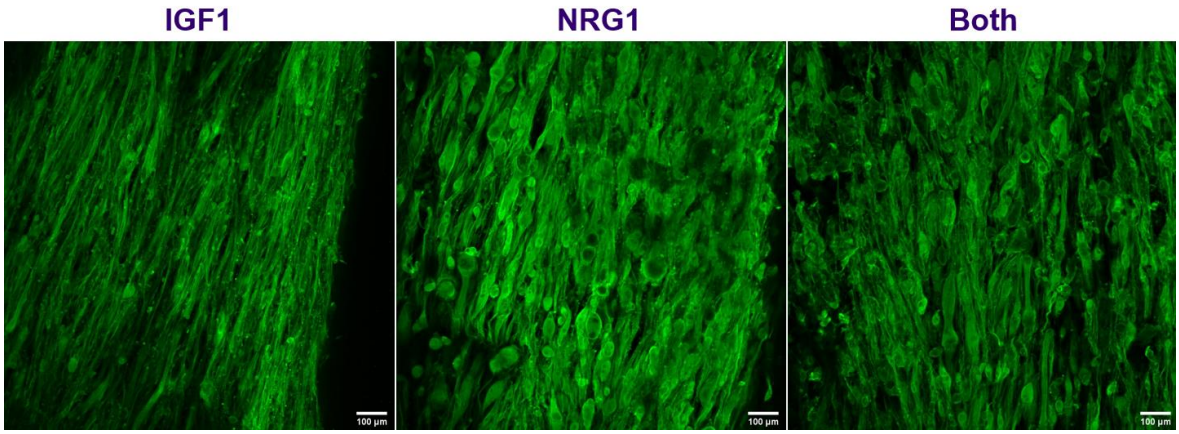

Fig #8: MyH7b staining of EMTs treated with IGF1 (left), NRG1 (middle), and both IGF1 and NRG1 (right) at 20x magnification.

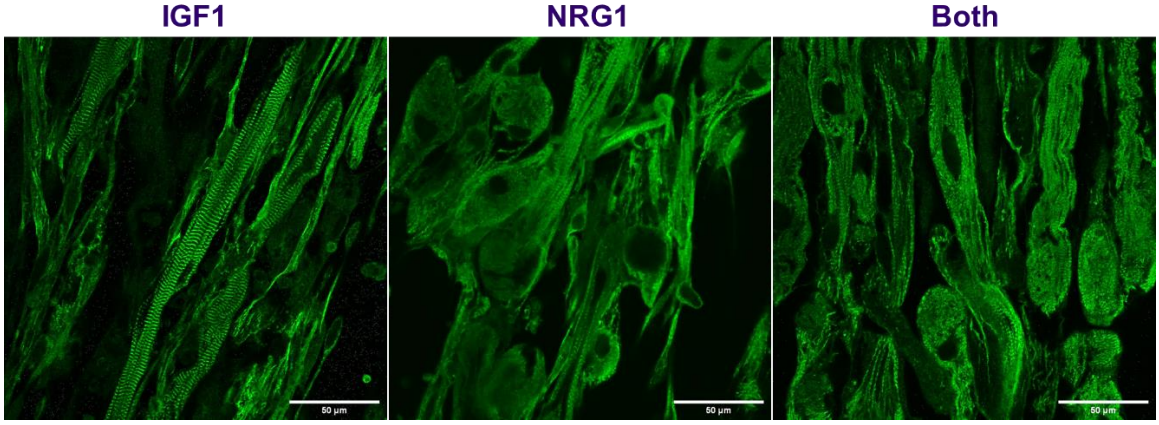

Fig #9: MyH7b staining of EMTs treated with IGF1 (left), NRG1 (middle), and both IGF1 and NRG1 (right) at 60x magnification.

I decided to attempt staining the EMTs again, but with alpha-actinin and a fresh nuclei stain (dapi). I performed this stain on EMTs fixed on Day 7 and Day 28 to assess differences in morphology at different timepoints in development. Again, these tissues were imaged at 20x magnification **(Fig#10)** and 60x magnification **(Fig#11).** At the day 7 timepoint, there is not an apparent difference in myotube appearance between the NRG1 treated EMTs and the controls at 20x. At 60x magnification, I can see sarcomere structures in both NRG1 treated and control EMTs. In the day 28 EMTs, while I see the same thin myotubes with well-defined sarcomere

structures in control EMTs, while I see large, bag-like myotubes and degrading sarcomere structures in NRG1 treated EMTs.

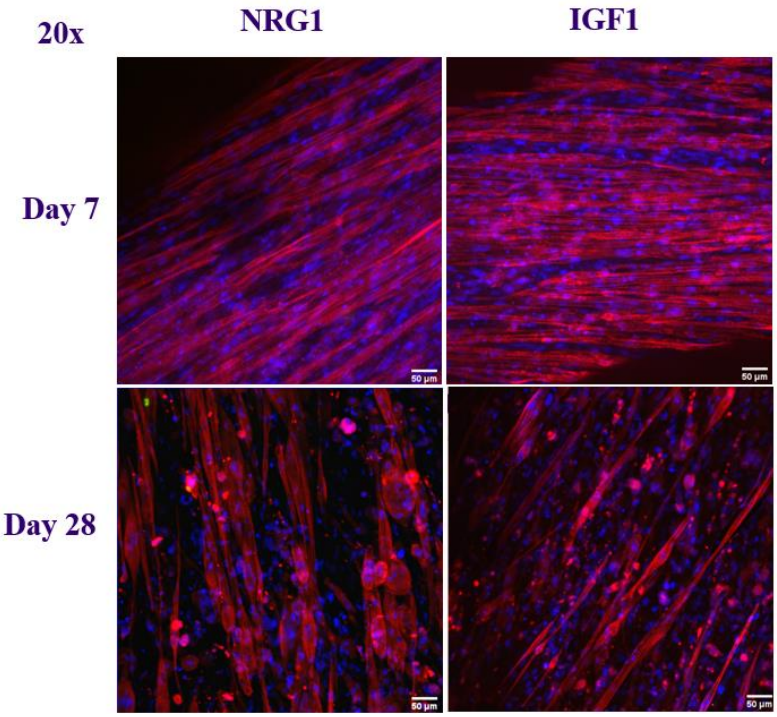

Fig #10: a-actinin staining of EMTs treated with IGF1 (right), NRG1 (left), at Day 7 (top) and Day 28 (bottom) at 20x magnification.

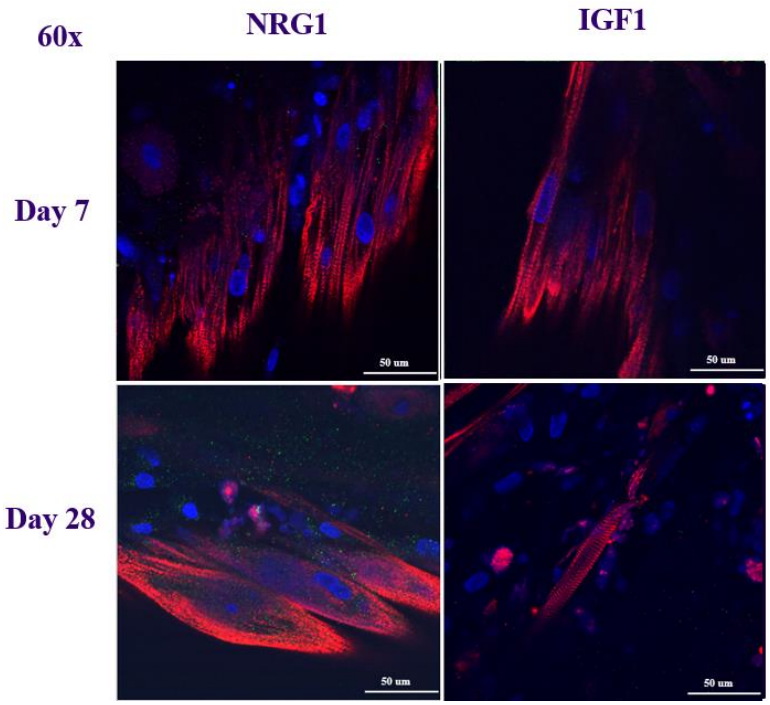

Fig #11: a-actinin staining of EMTs treated with IGF1 (right), NRG1 (left), at Day 7 (top) and Day 28 (bottom) at 60x magnification.

Based on the images took of the MyH7b and a-actinin stained EMTs, I used ImageJ to measure myotube width and sarcomere length. Results from this analysis showed that in conditions where NRG1 is present, there is a significant increase in myotube width as well as a significant decrease in sarcomere length **(Fig#12).**

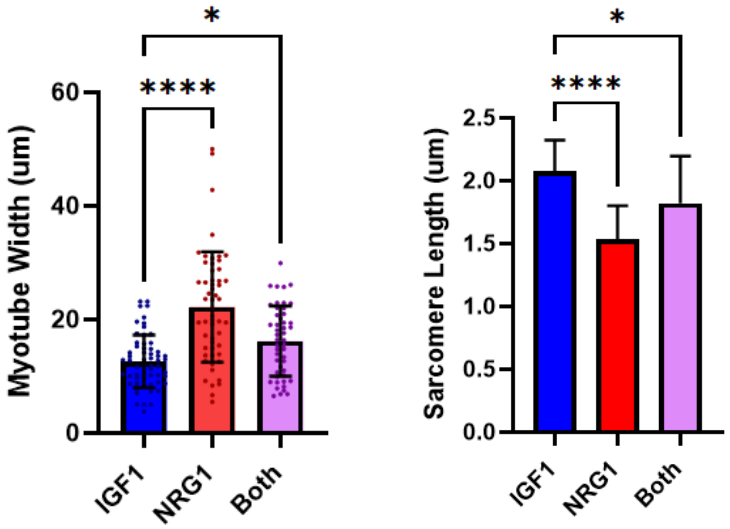

Fig #12: Quantification of EMT morphology based on myotube width (left) and sarcomere length (right). Myotube width: n=60 for all conditions, ****= p<0.0001, *=p=0.02. Sarcomere length: n=30 for all conditions, ****=p<0.0001, *=p=0.0405.

Function

The next section will address how the function of the EMTs was characterized. Force recordings of EMT contraction were taken on days 7, 10, 12, 14, 21, and 28. At these times, two broad-field stimulation protocols were run, the first being 5ms, 10V electrical pulses at a rate of 1Hz. This protocol allowed us to analyze twitch contractions of the muscle tissues over time.

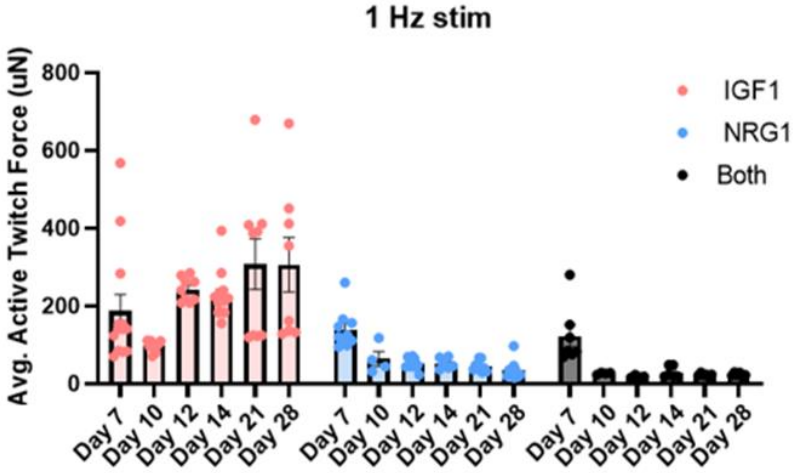

Fig #13: Average active twitch force over time from EMTs treated with IGF1 (red), NRG1 (blue), and both IGF1 and NRG1 (black).

The twitch force over time in the control EMTs (IGF1 condition) had a wide range, but maintained an average twitch force over 200uN past day 14 **(Fig #13).** In the two conditions where NRG1 is present, the trend is the same in that their twitch force is similar to controls at day 7, then has a major and consistent reduction in force production following. This protocol was also applied on EMTs being treated with varying concentrations of NRG1; 10ng/ml, 50ng/ml, and 100ng/ml. The trend was very similar between conditions, being the highest twitch force was measured on day 7, the lowest twitch force recorded on day 12, then the twitch force slightly increasing through day 28 **(Fig #14).**

Fig #14: Average active twitch force over time from EMTs treated with 10 ng/ml, 50ng/ml, and 100ng/ml of NRG1.

The second broad-field stimulation protocol applied to the EMTs was 5ms, 10V electrical impulses at frequencies of 1, 2, 3, 5, 10, 20, 30, 40, and 50 Hz. This protocol allowed us to analyze tetanic responses and force-frequency relationship of the EMTs over time. The IGF1 control EMTs produced tetanic contraction forces near 500uN over time **(Fig#15).** The NRG1 treated EMTs produced much less force throughout the protocol, hovering around 200uN at tetanus on days 7 and 14 then dropping in force production further at days 21 and 28. Additionally, on days 7 and 14, the NRG1 and both conditions did not exactly follow the sigmoidal force-frequency relationship that is expected.

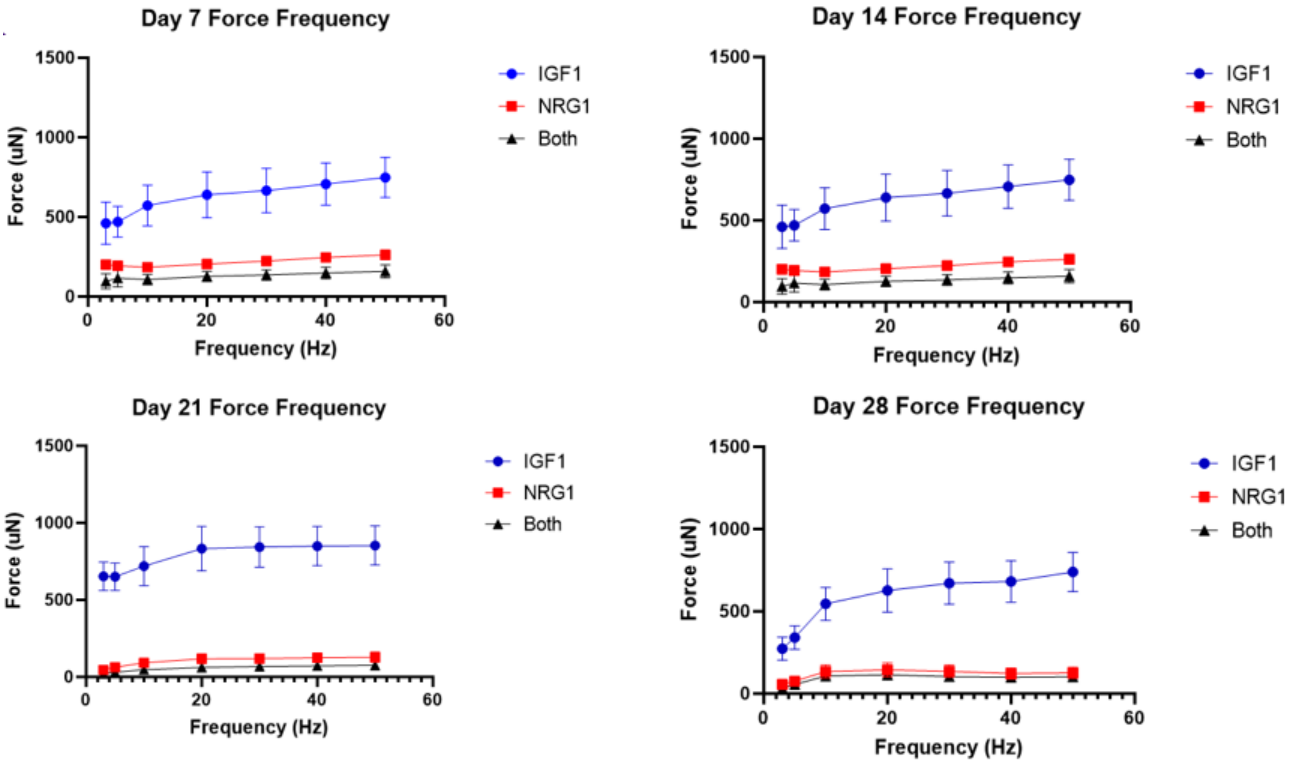

Fig#15: Force frequency curves over time from EMTs treated with IGF1 (blue), NRG1 (red), and both IGF1 and NRG1 (black). Error bars show SEM.

Discussion

There is a significant need to develop *in vitro* models of muscle spindles to better our general understanding of their development and function. Specifically, we need models of intrafusal spindle fibers so that we can understand how they act within the sensory reflex arc in the body and how they dysfunction in various disease states. This study aimed to investigate *de novo* intrafusal fiber induction protocols in 3D space. Through the use of a recombinant protein NRG1, skeletal muscle myoblasts receive a signal *in vitro* similar to how the signal is released by proprioceptive sensory afferents *in vivo*. As discussed previously, there has been work done previously investigating NRG1 treatment in 2D in rodent cells, primary human cells, and limited studies using iPS cells [11,14-16]. Previous work of my own using these cell types can be reviewed in the supplement **(Fig#S1-3)**. Briefly, I used C2C12 mouse skeletal muscle myoblasts as well as human-derived iPSCs in 2D to replicate intrafusal spindle fiber differentiation protocols. Through this work I found an increase in bag-like myotubes as well as specific Egr3 staining post-differentiation. This study aimed to build upon previous work to investigate and characterize this treatment using iPS cells in 3D space. As no 3D studies in the realm of muscle spindle research have been published, this work provides novel information about intrafusal fiber induction *in vitro*.

Due to limited research into muscle spindles, I first wanted to search through the literature to find and test antibody markers that would be intrafusal fiber specific. I planned to

apply these markers to sectioned rat soleus muscles and if any of them stained intrafusal fiber structures with specificity, I could use them as controls and then apply them to engineered muscle tissues. Multiple stains were attempted, and unfortunately, had very limited success. None of the antibody markers that were supposed to be intrafusal fiber specific stained positively across all structures. In addition, I saw very strange staining patterns when performing the MyL2 and MyH6 stains. This pattern showed tiger print-like staining across myotubes that I am unable to justify. These results suggest that the staining process needs to be optimized (i.e., more precise serum matching, more thorough wash steps to aid in clearance, different antibodies from different vendors) and also possibly the sectioning process needs to be optimized. As the sectioning was performed by the Histology Core at ISCRM, I want to attempt the process by myself to reduce outside factors when determining how best to optimize these processes.

One positive result obtained through this staining process was that I was able to identify an average of 8-10 spindles per soleus muscle. This is consistent with previous work regarding *in vivo* muscle spindles [29]. This gave me the confidence that I knew what I was looking at in terms of spindle structures, just that the antibodies and staining process was unsuccessful. Next, to actually investigate *de novo* intrafusal fiber formation *in vitro*, I generated EMTs from human-derived induced pluripotent stem cells. These cells give many advantages, including reducing ethical concerns, they are said to be infinitely expandable, and they give models increased translatability [42]. These EMTs were used to evaluate morphology, looking specifically at myotube and sarcomere structures, as well as function in terms of contractility and force generation. The EMTs, composed of myoblasts and dermal fibroblasts at casting, were treated with media including either NRG1, IGF1, or both. NRG1 treatment resulted in a significant increase in myotube width and a significant decrease in sarcomere length compared to controls EMTs. In NRG1 treated EMTs, I found more bag-like myotubes and within these myotubes, seemingly degrading sarcomere structures. This is consistent with previous work that has shown NRG1 is necessary for intrafusal fiber induction [5,12,14-16, 26-28].

When looking at the function of these EMTs, the first thing I looked at was twitch force. From this data I saw that NRG1 treatment led to a severe reduction in contractility and force production compared to the IGF1 controls. While the twitch force between conditions is roughly similar at day 7, at later timepoints the IGF1 controls have much greater force production. In addition, as the trend was the same between conditions where there was NRG1 only in the media and where both NRG1 and IGF1 are present, this led me to believe that the effects I was seeing were not due to a lack of IGF1, but rather the presence of NRG1.

These results called into question if the dose of NRG1 being applied to the EMTs (100ng/ml) was too concentrated and the reduction in contractility was due to toxicity effects. I then tested multiple concentrations of NRG1 (10, 50, and 100 ng/ml) and saw the exact same trend between concentrations. As the smaller concentrations of NRG1 had the same effect on function, and the 100ng/ml I used was based on work done by other groups, I could use a smaller concentration than previously established to achieve a similar effect on function. While this

experiment does not rule out NRG1 toxicity effects on the EMTs, it lessened the likelihood of this conclusion.

Next looking at the force frequency relationship and contraction force of then EMTs at tetanus, there is a similar trend in the data. The IGF1 control EMTs produced tetanic contraction forces near 500uN over time whereas the NRG1 treated EMTs produced around 200uN at tetanus on days 7 and 14, and even less on days 21 and 28. This data is supported by the observed decrease in sarcomere length, which would impede force production. Another interesting effect observed in the force-frequency curves of these EMTs, is that at early timepoints, NRG1 treatment generates more traditional contraction curves at tetanus **(Fig#S4).** NRG1 is obviously affecting the calcium handling of these cells, yet the exact mechanism in how it does this needs further investigation.

Future Directions

Due to the time constraints of this thesis, this project was intended to create a baseline in the Mack Lab in terms of understanding of muscle spindle development and *in vitro* spindle modeling. That being said, there are many directions of how this project could move forward. There are multiple experiments I believe would provide the most useful information and should be performed as the next steps. First would be to further investigate how timing of NRG1 application affects EMT morphology and force profiles. Introducing NRG1 at different timepoints (such as day 3, day 7, and day 14) would allow us to see how the presence of NRG1 at different points in muscle development affects intrafusal fiber induction. *In vivo*, NRG1 signaling occurs when sensory afferents contact developing myotubes. As the EMTs are cast with myoblasts, the more premature muscle cell type, it is possible that including NRG1 in the differentiation media at D0 may not be allowing for proper intrafusal fiber signaling to occur. In addition, NRG1 should be applied for various time increments (1 day, 3 days, and 7 days) to see if the length of time NRG1 is in the differentiation medium still shows the same effect that is observed. Does muscle recover if NRG1 is removed? Does any introduction of NRG1 start an irreversible change in phenotype?

The next experiment that would be worthwhile would be to perform spatial transcriptomic analysis. This method allows scientists to count the number of transcripts of a gene at distinct spatial locations in a tissue. I would apply this method to primary human spindle tissue, rodent spindle tissue, as well as the NRG1 treated and IGF1 control EMTs. This type of analysis would allow us to see what spindle genes are upregulated in rodent vs. human transcripts. In addition, it would allow us to see what genes are being upregulated in the EMTs so we can see where, if at all, in the intrafusal fiber differentiation pathway these tissues are at. Also, the data from this analysis should also be compared to the transcriptomic data from other groups such as the Kim lab and the Bornstein lab [30,31]. These two data sets are the only two publications to attempt in-depth spindle transcriptomics, but their results do not match up as expected, so performing our own in-house analysis could paint a clearer picture of what genes

are really present and relevant. This could also help us to identify more intrafusal fiber specific markers to test.

The next experiment I would recommend would be to co-culture the EMTs with afferent sensory neurons. In a co-culture system, the EMTs may receive more and/or different signals that may aid in their development toward becoming intrafusal spindle fibers. In addition, if we create these co-cultures, are we able to see the aunnulospiral wrappings that form around intrafusal fibers *in vivo*?

The last experiment I would recommend is to develop a stretch-based assay that can more accurately test intrafusal fiber function. While looking at contractility and force production gives us an idea of how the muscle cells are developing, the true test to see if these EMTs are becoming functional intrafusal fibers is to see if they have a functional response to stretch as that is how they are activated *in vivo*. One idea would be to still use the Mantarray system, but instead of using the magnetic sensing to view contractility, use the magnets to stretch the EMTs in the other direction, and perform live imaging to see if any signals are being sent.

Overall, this work provided novel information regarding intrafusal muscle spindle fiber development in 3D. It is the first study to monitor the contractility and force generation of NRG1 treated EMTs composed of human iPSC-derived myoblasts. This work will help advance muscle spindle research within the Mack Lab and the Neuromuscular Disease Research Group, and is part of the first steps toward generating an innervated muscle spindle in-a-dish model.

Acknowledgements

I would like to thank my P.I. David Mack, Ph.D., my mentor Alec Smith, Ph.D., the Neuromuscular Disease Research Group, and the Institute for Stem Cell and Regenerative Medicine for all of the help and guidance provided throughout this project.

Citation Disparity Statement

As a graduate student in research, I recognize citation disparities in literature where marginalized groups are under-cited relative to their quantity within the field and the quality of their work within the field. Within this work I have made efforts to cite articles that reflect the diversity within this area of work. I support and advocate for equitable practices in science, both in this publication and in future research

References

[1] Proske, U., Chen, B. Two senses of human limb position: methods of measurement and roles in proprioception. Exp Brain Res 239, 3157–3174 (2021). https://doi.org/10.1007/s00221-021-06207-4

[2] S. Kroger and B. Watkins, “Muscle spindle function in healthy and diseased muscle - skeletal muscle,” BioMed Central, 07-Jan-2021. [Online]. Available: https://skeletalmusclejournal.biomedcentral.com/articles/10.1186/s13395-020-00258-x.

[3]Kröger, Stephan. Proprioception 2.0: novel functions for muscle spindles. Current Opinion in Neurology 31(5):p 592-598, October 2018. | DOI: 10.1097/WCO.0000000000000590

[5] Oliveira Fernandes M, Tourtellotte WG. Egr3-dependent muscle spindle stretch receptor intrafusal muscle fiber differentiation and fusimotor innervation homeostasis. J Neurosci. 2015 Apr 8;35(14):5566-78. doi: 10.1523/JNEUROSCI.0241-15.2015. PMID: 25855173; PMCID: PMC4388921.

[6]Hippenmeyer S, Shneider NA, Birchmeier C, Burden SJ, Jessell TM, Arber S. A role for neuregulin1 signaling in muscle spindle differentiation. Neuron. 2002;36:1035–1049. doi: 10.1016/S0896-6273(02)01101-7.

[7]Leu M, Bellmunt E, Schwander M, Fariñas I, Brenner HR, Müller U. Erbb2 regulates neuromuscular synapse formation and is essential for muscle spindle development. Development. 2003;130:2291–2301. Doi:10.1242/dev00447.
[8] D. L. Falls, “Neuregulins and the neuromuscular system: 10 years of answers and questions,” J Neurocytol, vol. 32, no. 5–8, pp. 619–647, Jun. 2003, doi: 10.1023/B:NEUR.0000020614.83883.be.
[9] Ledonne, A.; Mercuri, N.B. On the Modulatory Roles of Neuregulins/ErbB Signaling on Synaptic Plasticity. Int. J. Mol. Sci. 2020, 21, 275. https://doi.org/10.3390/ijms21010275
[10] S. Hippenmeyer, N. A. Shneider, C. Birchmeier, S. J. Burden, T. M. Jessell, and S. Arber, “A role for neuregulin1 signaling in muscle spindle differentiation,” Neuron, vol. 36, no. 6, pp. 1035–1049, Dec. 2002, doi: 10.1016/s0896-6273(02)01101-7.
[11] M. Morano et al., “Modulation of the Neuregulin 1/ErbB system after skeletal muscle denervation and reinnervation,” Sci Rep, vol. 8, no. 1, p. 5047, Mar. 2018, doi: 10.1038/s41598-018-23454-8.
[12] Jacobson C, Duggan D and Fischbach G. Neuregulin induces the expression of transcription factors and myosin heavy chains typical of muscle spindles in cultured human muscle. Proc Natl Acad Sci 2004; 101: 12218–12223.
[13] J. Chal et al., "Generation of human muscle fibers and satellite-like cells from human pluripotent stem cells in vitro," (in eng), Nat Protoc, vol. 11, no. 10, pp. 1833-50, 10 2016, doi: 10.1038/nprot.2016.110.
[14] X. Guo et al., "Tissue engineering the mechanosensory circuit of the stretch reflex arc with human stem cells: Sensory neuron innervation of intrafusal muscle fibers," Biomaterials, vol. 122, pp. 179-187, 04 2017, doi: 10.1016/j.biomaterials.2017.01.005.
[15] A. Colón, X. Guo, N. Akanda, Y. Cai, and J. J. Hickman, "Functional analysis of human intrafusal fiber innervation by human γ-motoneurons," (in eng), Sci Rep, vol. 7, no. 1, p. 17202, 12 2017, doi: 10.1038/s41598-017-17382-2
[16]A. Colón, A. Badu-Mensah, X. Guo, A. Goswami, and J. J. Hickman, "Differentiation of Intrafusal Fibers from Human Induced Pluripotent Stem Cells," (in eng), ACS Chem Neurosci, vol. 11, no. 7, pp. 1085-1092, 04 2020, doi: 10.1021/acschemneuro.0c00055.
[17] Walro JM and Kucera J. Why adult mammalian intrafusal and extrafusal fibers contain different myosin heavy-chain isoforms. Trends Neurosci 1999; 22: 180–184.
[18] Pedrosa F, Soukup T and Thornell L-E. Expression of an alpha cardiac-like myosin heavy chain in muscle spindle fibres. Histochemistry 1990; 95: 105–113.
[19] Kucera J, Walro JM and Gorza L. Expression of type-specific MHC isoforms in rat intrafusal muscle fibers. Jourd Histochem Cytochem 1992; 40: 293–307.
[20] P. Barrett, T. J. Quick, V. Mudera, and D. J. Player, “Generating intrafusal skeletal muscle fibres in vitro: Current state of the art and future challenges,” Journal of tissue engineering, 29-Dec-2020. [Online]. Available: https://www.ncbi.nlm.nih.gov/pmc/articles/PMC8693220/.
[21] G. James *et al.*, “Muscle spindles of the multifidus muscle undergo structural change after intervertebral disc degeneration,” *Eur Spine J*, vol. 31, no. 7, pp. 1879–1888, Jul. 2022, doi: 10.1007/s00586-022-07235-6.
[22] C. Fan *et al.*, “Age-Related Alterations of Hyaluronan and Collagen in Extracellular Matrix of the Muscle Spindles,” *Journal of Clinical Medicine*, vol. 11, no. 1, Art. no. 1, Jan. 2022, doi: 10.3390/jcm11010086.
[23] K. Asano *et al.*, “Muscle spindle reinnervation using transplanted embryonic dorsal root ganglion cells after peripheral nerve transection in rats,” *Cell Prolif*, vol. 52, no. 5, p. E12660, Sep. 2019, doi: 10.1111/cpr.12660.
[24] M. Oliveira Fernandes and W. G. Tourtellotte, “Egr3-dependent muscle spindle stretch receptor intrafusal muscle fiber differentiation and fusimotor innervation homeostasis,” *J Neurosci*, vol. 35, no. 14, pp. 5566–5578, Apr. 2015, doi: 10.1523/JNEUROSCI.0241-15.2015.
[25] Y. Albert, J. Whitehead, L. Eldredge, J. Carter, X. Gao, and W. G. Tourtellotte, “Transcriptional regulation of myotube fate specification and intrafusal muscle fiber morphogenesis,” *J Cell Biol*, vol. 169, no. 2, pp. 257–268, Apr. 2005, doi: 10.1083/jcb.200501156.
[26] [1] J. W. Rumsey, M. Das, J.-F. Kang, R. Wagner, P. Molnar, and J. J. Hickman, “Tissue engineering intrafusal fibers: dose- and time-dependent differentiation of nuclear bag fibers in a defined in vitro system using neuregulin 1-beta-1,” Biomaterials, vol. 29, no. 8, pp. 994–1004, Mar. 2008, doi: 10.1016/j.biomaterials.2007.10.042.
[27] Herndon, C. A., Ankenbruck, N., and Fromm, L. (2014). The Erk MAP Kinase Pathway Is Activated at Muscle Spindles and Is Required for Induction of the Muscle Spindle-specific Gene Egr3 by Neuregulin1. J. Neurosci. Res. 92, 174–184. doi:10.1002/jnr.23293

[28] Akay, T., Tourtellotte, W. G., Arber, S., and Jessell, T. M. (2014). Degradation of Mouse Locomotor Pattern in the Absence of Proprioceptive Sensory Feedback. Proc. Natl. Acad. Sci. USA 111, 16877–16882. doi:10.1073/pnas.1419045111
[29] W. Lian et al., "Distribution Heterogeneity of Muscle Spindles Across Skeletal Muscles of Lower Extremities in C57BL/6 Mice," Front Neuroanat, vol. 16, p. 838951, 2022, doi: 10.3389/fnana.2022.838951.
[30] B. Bornstein et al., "Molecular characterization of the intact muscle spindle using a multi-omics approach," Developmental Biology, preprint, Jul. 2022. doi: 10.1101/2022.07.13.499888.
[31] M. Kim et al., "Single-nucleus transcriptomics reveals functional compartmentalization in syncytial skeletal muscle cells," Nat Commun, vol. 11, no. 1, p. 6375, Dec. 2020, doi: 10.1038/s41467-020-20064-9.
[32] J. Appl. Phys. 127, 194701 (2020); https://doi.org/10.1063/1.5129347 Submitted: 27 September 2019 • Accepted: 21 April 2020 • Published Online: 19 May 2020
[33] Chal J, Al Tanoury Z, Hestin M, et al. Generation of human muscle fibers and satellite-like cells from human pluripotent stem cells in vitro. Nat Protoc 2016; 11: 1833–1850. Crossref. PubMed.
[34] Chal J, Oginuma M, Al Tanoury Z, et al. Differentiation of pluripotent stem cells to muscle fiber to model Duchenne muscular dystrophy. Nat Biotechnol 2015; 33: 962–969. Crossref. PubMed.
[35] C. A. Herndon, N. Ankenbruck, B. Lester, J. Bailey, and L. Fromm, "Neuregulin1 signaling targets SRF and CREB and activates the muscle spindle-specific gene Egr3 through a composite SRF-CREB-binding site," Exp Cell Res, vol. 319, no. 5, pp. 718–730, Mar. 2013, doi: 10.1016/j.yexcr.2013.01.001.
[36] Y. Qiao, M. Cong, J. Li, H. Li, and Z. Li, "The effects of neuregulin-1β on intrafusal muscle fiber formation in neuromuscular coculture of dorsal root ganglion explants and skeletal muscle cells," Skelet Muscle, vol. 8, no. 1, p. 29, Sep. 2018, doi: 10.1186/s13395-018-0175-9.
[37] C. Cheret et al., "Bace1 and Neuregulin-1 cooperate to control formation and maintenance of muscle spindles," EMBO J, vol. 32, no. 14, pp. 2015–2028, Jul. 2013, doi: 10.1038/emboj.2013.146.
[38] D. L. Falls, "Neuregulins and the neuromuscular system: 10 years of answers and questions," J Neurocytol, vol. 32, no. 5–8, pp. 619–647, Jun. 2003, doi: 10.1023/B:NEUR.0000020614.83883.be.
[39] B. D. Ford, B. Han, and G. D. Fischbach, "Differentiation-dependent regulation of skeletal myogenesis by neuregulin-1," Biochem Biophys Res Commun, vol. 306, no. 1, pp. 276–281, Jun. 2003, doi: 10.1016/s0006-291x(03)00964-1.
[40] B. Kowalczyk and J. Feluś, "Arthrogryposis: an update on clinical aspects, etiology, and treatment strategies," Arch Med Sci, vol. 12, no. 1, pp. 10–24, Feb. 2016, doi: 10.5114/aoms.2016.57578.
[41] D. Desai, D. Stiene, T. Song, and S. Sadayappan, "Distal Arthrogryposis and Lethal Congenital Contracture Syndrome - An Overview," Front Physiol, vol. 11, p. 689, 2020, doi: 10.3389/fphys.2020.00689.
[42] Shi Y, Inoue H, Wu JC, Yamanaka S. Induced pluripotent stem cell technology: a decade of progress. Nat Rev Drug Discov. 2017 Feb;16(2):115-130. doi: 10.1038/nrd.2016.245. Epub 2016 Dec 16. PMID: 27980341; PMCID: PMC6416143.

Supplement

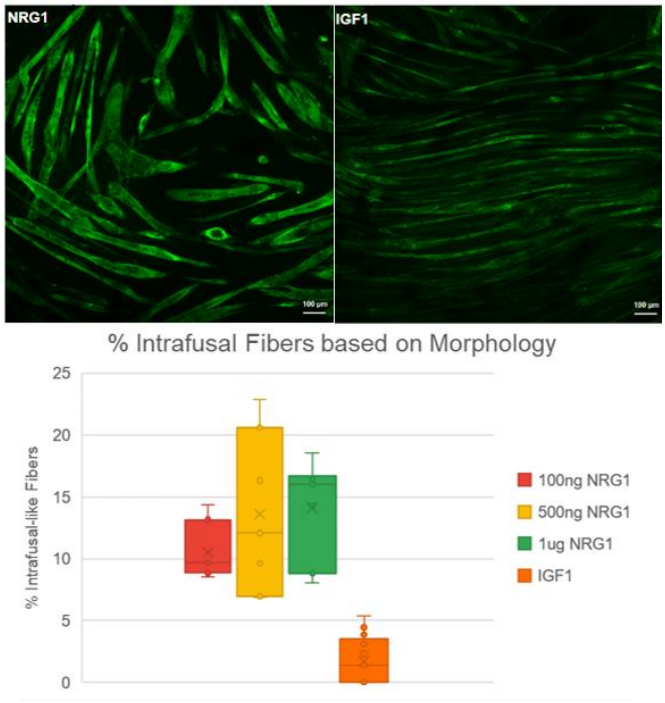

Fig #S1: C2C12 cells treated with NRG1 (left) and IGF1 (right), stained with a fast Myosin Heavy Chain antibody. Results from C2C12 experiments as determined by morphological analysis (bottom)

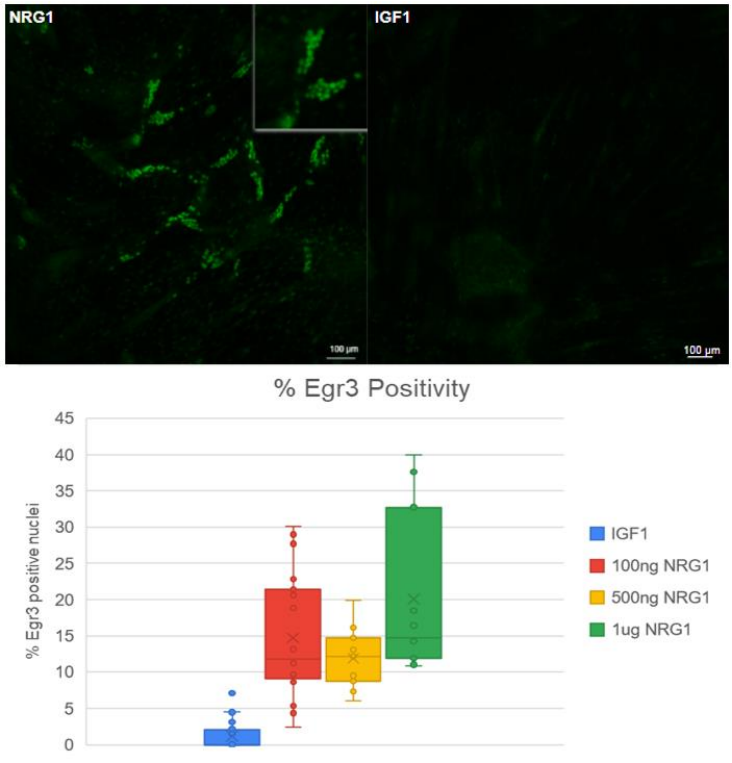

Fig #S2: C2C12 cells treated with NRG1 (left) and IGF1 (middle), stained with an Egr3 antibody. Results from experiments as determined by the percent of total nuclei that stained positive for Egr3 (bottom).

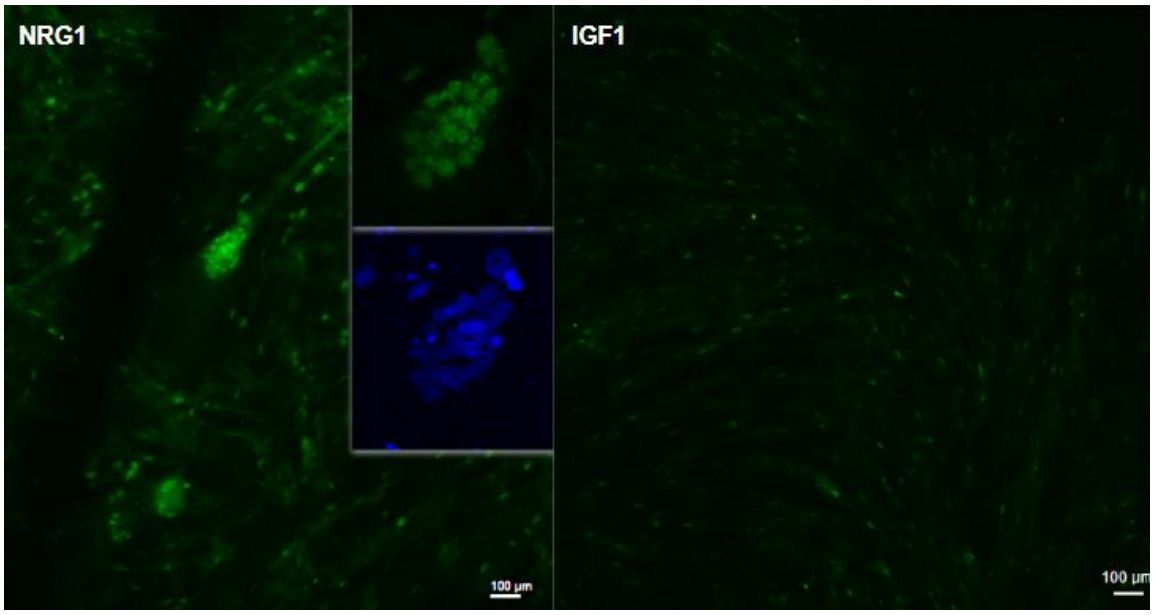

Fig #S3: Induced pluripotent stem cells treated with NRG1 (left) and IGF1 (right) stained with the Egr3 antibody.

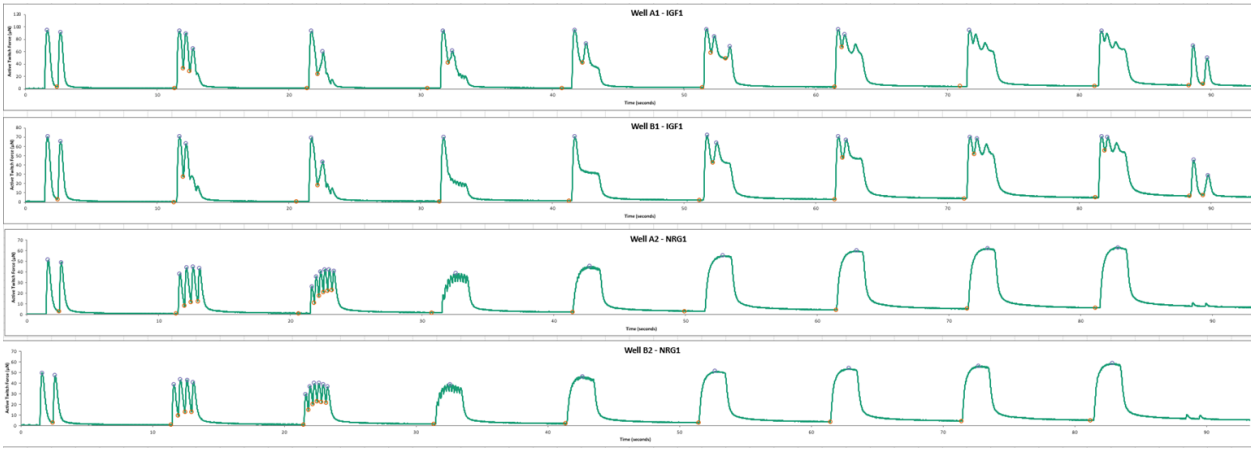

Fig #S4: Representative Day 7 contraction force tracings of control EMTs (top two tracings) compared to NRG1 treated EMTs (bottom two tracings).